J Mol Med (2013) 91:117–128
DOI 10.1007/s00109-012-0940-x

JMolMed

ORIGINAL ARTICLE

Functionalized single-walled carbon nanotubes cause reversible acute lung injury and induce fibrosis in mice

Yanli Zhang · Jiejie Deng · Yanxu Zhang · Feng Guo · Chenggang Li · Zhen Zou · Wen Xi · Jun Tang · Yang Sun · Peng Yang · Zongsheng Han · Dangsheng Li · Chengyu Jiang

Received: 16 November 2011 / Revised: 25 July 2012 / Accepted: 27 July 2012 / Published online: 10 August 2012

Abstract Nanotechnology is one of today's most promising technological developments, but safety concerns raise questions about its development. Risk assessments of nanomaterials during occupational exposure are crucial for their development. Here, we assessed the lung toxicity of functionalized single-walled carbon nanotube (f-SWCNT) exposure in C57BL/6 mice, elucidated the underlying molecular mechanism, and evaluated the self-repair ability and lung fibrosis of the mice. Soluble f-SWCNTs were administered to mice. After 18 h or 14 days, the lung histopathology, bronchoalveolar lavage fluid, lung edema, vascular permeability, and PaO_2 levels were evaluated, and biochemical and immunostaining tests were also performed. We found that some f-SWCNTs could induce acute lung injury (ALI) in mice via proinflammatory cytokine storm signaling through the NF-κB pathway in vivo. We illustrated that corticosteroid treatments could ameliorate the ALI induced by the f-SWCNTs in mice. Surprisingly, the ALI was almost completely reversed within 14 days, while mild to moderate fibrosis, granuloma, and DNA damage remained in the mice at day 14. Our studies indicate potential remedies to address the growing concerns about the safety of nanomaterials. In addition, we notify that the type of functional groups should be considered in nanomedicine application as differently functionalized SWCNTs generated different effects on the lung toxicity.

Keywords Acute lung injury · Dexamethasone · f-SWCNTs · Fibrosis · NF-κB

Y. Zhang and J. Deng contributed equally to this work.

Electronic supplementary material The online version of this article (doi:10.1007/s00109-012-0940-x) contains supplementary material, which is available to authorized users.

Y. Zhang · J. Deng · Y. Zhang · F. Guo · C. Li · Z. Zou · W. Xi · J. Tang · Y. Sun · P. Yang · Z. Han · C. Jiang (✉)
State Key Laboratory of Medical Molecular Biology, Department of Biochemistry and Molecular Biology, Institute of Basic Medical Sciences, Chinese Academy of Medical Sciences, Peking Union Medical College, Tsinghua University,
Chengyu Jiang, Room 460, No. 5 Dongdansantiao,
Beijing 100005, China
e-mail: chengyujiang@gmail.com

D. Li
Shanghai Institutes for Biological Sciences,
Chinese Academy of Sciences,
Shanghai 200031, China

Introduction

Human acute and chronic lung injuries resulting from exposure to nanoparticles or ultrafine particles have been reported for decades in occupational or environmental settings, but the underlying molecular mechanisms remain unclear [1–3]. Carbon nanotubes are one of the most prominent nanomaterials [4–6], mainly consisting of multi- (MWCNTs) and single-walled carbon nanotubes (SWCNTs). Previous studies reported that MWCNTs could induce toxicity both in vitro and in vivo [7, 8]. Recent studies have shown that the administration of clinical doses of soluble MWCNTs in mice could cause reversible testis damage without affecting fertility [9]. SWCNTs, with their special one-dimensional nanostructure and unique properties, are currently of great interest for a variety of applications, especially for biomedical applications. SWCNTs can be easily and accessibly functionalized to become soluble and used as versatile excipients in nanomedicine for drug delivery and disease imaging, suggesting an important role

in the treatment and monitoring of diseases [4–6, 10, 11]. As an example of functionalized SWCNT (f-SWCNT) use in drug delivery, paclitaxel (PTX) was conjugated to poly(ethylene glycol)-functionalized SWCNT (PEG-SWCNT) via a cleavable ester bond to obtain a water-soluble f-SWCNT-PTX conjugate, which afforded higher efficacy in suppressing tumor growth than clinical Taxol in a murine cancer model [10]. Although controversial toxic results have been reported from insoluble pristine SWCNT studies in vivo and in vitro [12–15] and soluble f-SWCNT studies in immune [16], neuronal cells [17], and mouse liver [18], the pulmonary toxicity studies on soluble f-SWCNTs have not been systematically reported in vivo [19–21]. Konduru et al. [19] described phosphatidylserine (PS) coated SWCNTs enhanced uptake by alveolar macrophages, and Tong et al. [20] showed AF-SWCNT had increased percentage of PMN and NAG in BAL with high dose of AF-SWCNT treatments. Our previous study also showed COOH modified SWCNT, but not PEG-SWCNT and PABS-SWCNT, induced autophagic cell death through Akt-TSC2-mTOR signal pathway [21]. However, most of the above experiments are performed in cells and lack direct evidences for pulmonary toxicity and lung injury in vivo. Moreover, there is a lack of comparison between the pulmonary toxicity of f-SWCNTs with varied functional groups in vivo.

The lung is the primary target for f-SWCNT toxicity because with sufficient agitation, SWCNT material can release fine particles into the air to a peak airborne concentration of 53 $\mu g/m^3$, which thus can easily be inhaled during production or utilization [22]. This observation emphasizes the importance of evaluating the pulmonary toxicity of f-SWCNTs. The initiation of an inflammatory response has primarily been observed following exposure to many nanoparticles [1, 23], and pristine insoluble SWCNTs have also been reported to be capable of inducing pulmonary inflammation and granuloma formation in vivo [13–15]. We have designed a mouse model using the intratracheal instillation of serial concentrations of modified f-SWCNTs to assess the induced pulmonary toxicity and inflammation. After 18 h or 14 days, we evaluated the effects of these exposures on the histopathology of the lung and examined the release of inflammatory mediators by alveolar macrophages, lung edema, vascular permeability, PaO_2 levels, lung fibrosis, and the activation of the inflammatory NF-κB signaling pathway in the lung.

Corticosteroids, immune modulators that have strong anti-inflammatory activities, are widely prescribed for many immune and inflammatory diseases [24]. Corticosteroids have also been used in the therapeutic treatments of acute lung injury (ALI) or acute respiratory distress syndrome (ARDS) [25]. We hypothesized that f-SWCNTs might induce ALI by causing excessive systemic inflammation. Dexamethasone and methylprednisolone, members of the corticosteroid class of hormones, were therefore administered to the f-SWCNT groups to assess their ability to suppress nanomaterial-induced lung injury.

The purpose of this study was to assess lung toxicity using serial concentrations of f-SWCNTs. Additionally, we sought to reveal the underlying mechanism of the ALI induced by f-SWCNTs with the goal of providing a useful recommendation for clinicians to use corticosteroids as potential agents to remedy the ALI induced by unintentional exposure to f-SWCNTs. Finally, we evaluated the self-repair ability and lung fibrosis of the mice after 14 days.

Materials and methods

Mice Transgenic mice with a luciferase reporter for NF-κB, BALB/C-Tg(NFκB-luc [Oslo])-Xen (5–6 weeks old, Caliper Life Sciences Inc., MA, USA), were used for the in vivo imaging analysis of luciferase activity. Only sex-, age-, and background-matched mice were used as controls. C57BL/6 mice (5–6 weeks old) were purchased from Vital River (Beijing, China). The weight of the mice used for f-SWCNT dosing was 15–17 g. The mice were housed under specific pathogen-free conditions. The mouse experiments were conducted in the animal facility at the Institute of Basic Medical Sciences of Peking Union Medical College in accordance with the governmental and institutional animal care and use committee guidelines.

f-SWCNTs solution preparation and characterization f-SWCNTs with a BET surface area of approximately 400 m^2/g (Sigma-Aldrich, St. Louis, MO, USA) were weighed and dissolved in sterilized ultrapure water at 5 mg/ml using sonication in a water bath until all material was completely dispersed according to visual observation. Then, the solution was centrifuged at 5,000×*g* for 5 min. The upper layer was collected and aliquoted, and its concentration was determined by drying a 1.000 ml aliquot completely in an Eppendorf tube at 65 °C for 24 h and weighing the dried SWCNTs using a Mettler MT5 microbalance (Mettler-Toledo, Hightstown, NJ, USA). The aliquots were sonicated for 10 min before later use. A volume of 60 μl of the above suspension adjusted to the appropriate concentrations or water was instilled per mouse. The suspensions were diluted to 0.1 mg/mL and examined with a transmission electron microscope (Tecnai G20, FEI Co., USA).

Reagents The fullerene-C60 (C60) and graphitized carbon black (mean particle size, 5 μm) with a mesoporous, hydrophilic pore surface and a BET surface area of 300 m^2/g were from Sigma-Aldrich (product number 702110, St. Louis, MO, USA). The phospho-IκB, total IκB, and β-actin antibodies were from Cell Signaling Technology® (Boston, MA, USA).

The NE-PER® Nuclear Extraction Reagents and Light Shift® Chemiluminescent electrophoretic mobility shift assay (EMSA) kit were from Thermo-Scientific PIERCE® (Rockford, IL, USA). The NF-κB oligonucleotide sequences, which were synthesized by Invitrogen (Carlsbad, CA, USA), were as follows: 5′-AGT TGA GGG GAC TTT CCC AGG C-3′ and 5′-G CCT GGG AAA GTC CCC TCA ACT-3′. The interleukin 6 (IL-6), tumor necrosis factor alpha (TNF-α), and IL-1β ELISA MAX™ Deluxe Sets were from Biolegend® (CA, USA). The dexamethasone and methylprednisolone were from Kingyork Company (Tianjin, China) and Pfizer Manufacturing Belgium NV (Puurs, Belgium), respectively.

f-SWCNT instillation, BAL, lung wet/dry ratio assay, and histopathological examination of mouse lung tissue The mice were randomly grouped. After anesthesia by an intraperitoneal injection of 1 % pentobarbital sodium solution, the mice were intratracheally instilled with water, f-SWCNTs, C60, or carbon black. Instillation was chosen here as the exposure method over other methods, such as inhalation and aspiration, because of the accuracy of the f-SWCNT intake during manipulation. After 18 h, the trachea was cannulated after anesthesia. The bronchoalveolar lavage fluid (BALF) was obtained by washing the lungs with 3× 0.8 ml of sterile ice-cold phosphate-buffered saline (PBS) and centrifuged at 400×*g* for 10 min at 4 °C. The supernatant from the first lavage was tested for the concentration of IL-6, TNF-α, and IL-1β. The total number of cells in the lavage fluid was counted with a hemocytometer. Cell differentials were counted from cytospin preparations stained with Wright–Giemsa stain using at least 200 cells per slide (M&C Gene Technology, Beijing, China). For Western blots of the BALF cells, the pelleted cells were lysed, denatured at 97°C for 10 min, and analyzed for IκB. The band density was calculated using Quantity One software. In the lung wet/dry ratio assay, which provides information on pulmonary edema, the mice were killed, and the wet weight of their lungs was measured. To obtain the dry weight, the lungs were dried at 65 °C for 24 h. For histopathological examination, lungs were fixed in formalin for 48 h and embedded in paraffin and 4-μm sections were stained with H&E. Micrographs were taken with a Leica DM3000 microscope using a Leica DFC 420 digital camera and Leica Qwin V3 software. The number of infiltrating cells was counted in 100 microscopic fields for each group at a magnification of 1,000×. The collagen content was detected by Masson's trichrome staining of lung sections. The percentages of fibrosis and granuloma area in the lung parenchyma were calculated using ImagePlus6.0 software. The granuloma numbers were determined by counting the number of granulomas present in each microscope picture. At least 100 fields were analyzed for fibrosis and granulomas in each lung at a magnification of 200×. Antibodies to α-SMA, collagen I and III were from Abcam (Cambrodge, MA, USA). The p-H2A.X antibody was from Bioworld Technology, Inc. (St. Louis Park, MN, USA). At least 20 fields in the f-SWCNT groups were analyzed for immunostaining in each lung at a magnification of 200×.

Blood oxygenation and pulmonary vascular permeability The blood samples were obtained from the common carotid artery, and the partial pressure of oxygen in the arterial blood (PaO_2) was measured. Pulmonary vascular permeability was assessed by measuring the pulmonary extravasation of Evans Blue. Evans Blue (20 μg/g) was injected into the angular vein 18 h after instillation, and 10 min after the injection of Evans Blue, the animals were killed. Lungs were then perfused with ice-cold PBS before the lung tissue was used to determine the content of Evans Blue.

In vivo imaging of luciferase activity D-Luciferin (120 mg/kg, Promega, Madison, WI, USA) dissolved in 200 μl PBS, pH 7.8, was injected into tail veins of the transgenic mice. Five minutes later, the mice were dissected, and lungs were placed in a lightproof chamber with an ultrasensitive camera positioned above. Grayscale images were taken for positional and landmark references. The luminescence emitted from the lungs was continuously recorded for 5 min and subsequently integrated by the software in our experimental apparatus (Berthold Technologies).

Electrophoretic mobility shift assay The lung tissues were harvested 18 h after AMIDE-SWCNT administration. Nuclear protein extracts were obtained from the lung tissues and used for EMSA according to the Thermo Scientific protocols.

Statistical analyses All data are shown as the mean±SEM. The statistical analyses were conducted using ANOVA analysis when comparing more than two groups and Student's *t* test for two groups.

Results

Characterization of f-SWCNTs After dissolution, sonification, and centrifugation, the upper layer suspensions were black and stable without obvious precipitation for more than 2 months. The characterization of the f-SWCNT solution by TEM showed that the f-SWCNTs dispersed well in water and retained the structural integrity of carbon nanotubes with a typical diameter of 1–2 nm and a length ranging from 500 to 1500 nm (Fig. S1).

f-SWCNTs can induce ALI through pro-inflammatory cytokines f-SWCNTs chemically modified with an amide group,

a carboxyl group (COOH), a polyaminobenzene sulfonic acid group (PABS), or a PEG group, which are biocompatible and have great potential for use in biomedicine, were used in our experiments [4–6, 10, 11]. To assess pulmonary toxicity, we intratracheally administered the f-SWCNTs at 0, 0.06, 0.2, 0.6, 2, and 10 mg/kg to mice and analyzed the histopathology of the lungs. These concentrations were chosen with the aim of generally covering a range of concentrations that would induce different degrees of lung injury, from minor to severe. Representative micrographs from each group 18 h after f-SWCNT instillation are shown (Fig. 1a). More severe inflammation and a larger quantity of infiltrating cells were observed in the 0.6, 2, and 10 mg/kg f-SWCNT-treated groups compared with the control groups (Fig. 1a, b). The instilled dosage correlated with the degree of inflammatory response to the f-SWCNTs. The f-SWCNT doses of <0.6 mg/kg instilled in mice caused little harm to the lungs (Fig. 1a, b).

To further analyze the inflammation and the inflammatory cell influx into the lungs, we performed BALF cell differentiation and cytokine detection after the intratracheal instillation of serial concentrations (0, 0.06, 0.2, 0.6, 2, and 10 mg/kg) of the f-SWCNTs. The total inflammatory cells in the BALF were increased significantly and dose-dependently in the 0.6, 2, and 10 mg/kg f-SWCNT-treated groups compared with the control groups (Fig. 1c). The PMN influx into the airspace, known as the most sensitive and sound parameter of acute inflammation, also increased significantly and dose-dependently in the 0.6, 2, and 10 mg/kg f-SWCNT-treated groups, composing the major contributing factor to the rapid increase in the total cell count. Especially, when comparing the four differently functionalized SWCNTs, AMIDE-SWCNT group exhibited the maximum increment in PMN counts (Fig. 1d). The lymphocyte numbers reached their maximum levels in the 10 mg/kg f-SWCNT-treated groups (Fig. 1e). Although the percentage of macrophages dropped

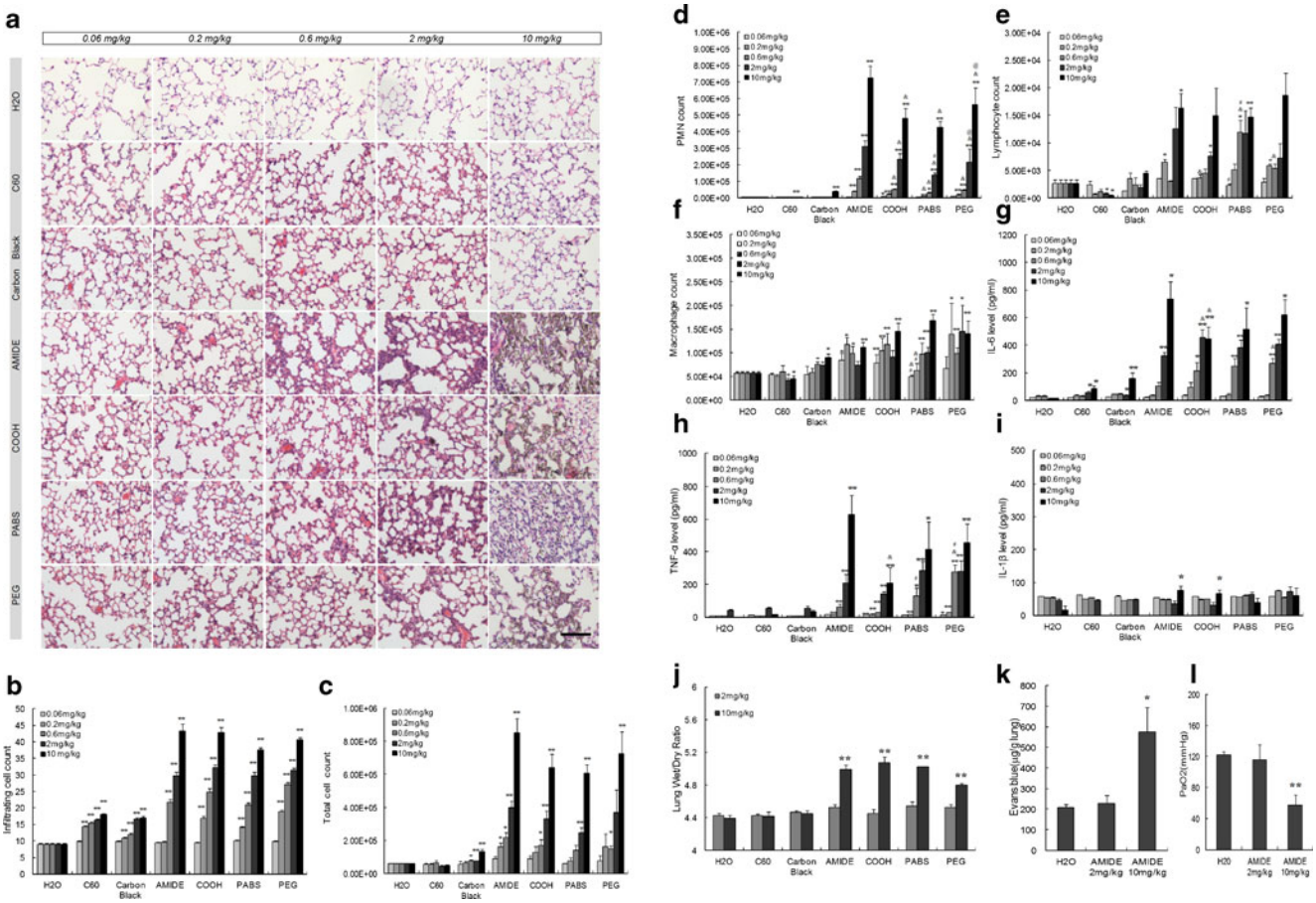

Fig. 1 Pulmonary pathologic, BALF, and functional analyses of mice 18 h after the instillation of f-SWCNTs. The mice were intratracheally given water, f-SWCNTs, C60, or carbon black at **a–h** 0, 0.06, 0.2, 0.6, 2, and 10 mg/kg or **i–k** 0, 2, and 10 mg/kg, respectively. **a** Representative H&E-stained lung sections from mice. **b** Statistical analysis of the infiltrating cell numbers. **C–h** Analysis of the BALF collected 18 h after instillation using Wright–Giemsa staining under light microscopy: total cell count (**c**), PMN count (**d**), lymphocyte count (**e**), and macrophage count (**f**). **g–i** ELISA analysis of the BALF: IL-6 (**g**), TNF-α (**h**), and IL-1β (**i**). **j–l** Analysis of the f-SWCNT-induced lung injury: lung wet/dry ratios (**j**), Evans blue staining (**k**), and PaO_2 (**l**). n=4–6 per group. *P<0.05, **P<0.01 versus control. $^{\&}P$<0.05, $^{\#}P$<0.05, $^{@}P$< 0.05 versus corresponding concentration of AMIDE-SWCNT, COOH-SWCNT, and PABS-SWCNT, respectively. Scale bar, 100 μm

sharply from >90 % to <20 %, the absolute value significantly increased in most of the f-SWCNT-treated groups (Fig. 1f). The lung was reported to be a major source of the cytokine storm in those patients with an inflammatory lung process [26]. Alveolar macrophages secrete cytokines, including the proinflammatory cytokines IL-6 and TNF-α, which are the primary contributors to hypercytokinemia. Therefore, we analyzed the expression of IL-6, TNF-α and IL-1β in the BALF. The concentrations of secreted IL-6 and TNF-α in the BALF were significantly upregulated, a sign of alveolar macrophage activation, in the groups that received 0.6, 2, and 10 mg/kg f-SWCNTs in a dose-dependent manner (Fig. 1g, h). The concentrations of IL-6 and TNF-α were 51- and 66-fold higher, respectively, in the group that received 10 mg/kg AMIDE-SWCNT compared with the control group. IL-6 and TNF-α were not significantly elevated in the BALF of the 0.06 and 0.2 mg/kg groups compared with the control (Fig. 1g, h). IL-1β increased significantly in the BALF of the 10 mg/kg AMDIE-SWCNT and COOH-SWCNT groups compared with the control (Fig. 1i). These results suggested that f-SWCNT doses of or higher than 0.6 mg/kg induced the production of pro-inflammatory cytokines, which may cause a cytokine storm and lead to ALI in mice.

To further assess the pulmonary toxicity, we intratracheally instilled the different f-SWCNTs at 0, 2, and 10 mg/kg into mice and analyzed the wet/dry weight ratios of the lungs as a marker of pulmonary edema. The mouse lung wet/dry weight ratios of the 10 mg/kg f-SWCNT group were significantly higher than those of the control groups. Although the wet/dry weight ratios increased in the 2 mg/kg f-SWCNTs group compared with the control mice, the differences were not statistically significant (Fig. 1j). We also examined whether the AMIDE-SWCNT treatment resulted in enhanced pulmonary vascular permeability, a hallmark of ALI in humans, using Evans Blue dye injections as an in vivo assay of albumin leakage. The instillation of 10 mg/kg AMIDE-SWCNT increased vascular permeability significantly (Fig. 1k). PaO_2, an indicator of respiratory failure, was measured to assess arterial blood oxygenation. Mice treated with AMIDE-SWCNT at 10 mg/kg showed significantly decreased PaO_2 (Fig. 1l). No significant differences were detected in the 2 mg/kg AMIDE-SWCNT group (Fig. 1k, l). The mice given C60 and carbon black showed no ALI and rather small changes in the numbers of BALF infiltrating cells and levels of cytokines (Fig. 1a–j). In summary, these results showed that f-SWCNTs at a dose above 0.6 mg/kg resulted in lung toxicity. Moreover, the mice exposed to more than 10 mg/kg AMIDE-SWCNT developed ALI.

f-SWCNTs induce mouse ALI through the NF-κB-cytokine signaling pathway NF-κB is a key player in the inflammatory response. We hypothesized that activation of NF-κB may be responsible for the increased proinflammatory cytokine storm induced by the f-SWCNTs. Previous studies have shown that the exposure to pristine SWCNTs induced the activation of NF-κB in human keratinocytes [12] and monocytic leukemia cells [13] in vitro, but until now, no integrated signal pathway has been shown to be responsible for the activation of NF-κB by pristine SWCNTs, let alone the f-SWCNTs in vivo. We first examined the activation of NF-κB in response to f-SWCNT instillation in vivo using a transgenic mouse model harboring a luciferase reporter controlled by NF-κB. A remarkable level of luciferase activity, as measured by bioluminescence imaging, was found in the lungs of the transgenic mice instilled with AMIDE-SWCNT (Fig. 2a, lower panel), indicative of NF-κB activation. In contrast, no bioluminescent signal could be observed in the water-treated transgenic mouse (Fig. 2a, upper panel). EMSA analysis indicated that the AMIDE-SWCNT instillation increased the DNA binding activity of NF-κB in the nuclear extracts from the mouse lungs (Fig. 2b). Taken together, these results indicate that AMIDE-SWCNT activates NF-κB in vivo. Furthermore, the f-SWCNT instillation in mice induced the phosphorylation of IκB in the BALF macrophages (Fig. 2c), which would result in the subsequent proteolysis of IκB and activation of NF-κB.

In summary, these results suggested that the f-SWCNTs induced mouse ALI through the NF-κB-cytokine signaling pathway (Fig. 2d).

Corticosteroids ameliorate the mouse ALI induced by f-SWCNTs Previous reports have shown that corticosteroids reduce inflammation and affect the immune system [24]. We therefore speculated that corticosteroids might ameliorate the cytokine storm and ALI induced by the f-SWCNTs in vivo. We intratracheally administered the f-SWCNTs to mice and analyzed the BALF IL-6 levels and lung edema degree 18 h later, with an i.p. injection of the corticosteroids dexamethasone (10 mg/kg) or methylprednisolone (50 mg/kg) or the PBS vehicle 1 h before instillation of the f-SWCNTs. The BALF IL-6 levels and lung edema induced by the f-SWCNTs were significantly reduced when the corticosteroids dexamethasone or methylprednisolone, respectively, were i.p. injected in mice (Fig. 3a, b). These results indicate that inflammation plays an important role in the f-SWCNT-induced ALI in mice and that these effects could be ameliorated by suppressing the proinflammatory cytokine levels with corticosteroid treatment in vivo (Fig. 3c).

f-SWCNTs cause reversible ALI and induce granuloma, fibrosis, and DNA damage in mice To examine the self-repair ability of the ALI in the mice challenged with a high dose of f-SWCNTs, we first assessed the ALI induced by 2 and 10 mg/kg AMIDE-SWCNT in mice without any treatments after 2 weeks. Surprisingly, the symptoms of the ALI were almost completely recovered

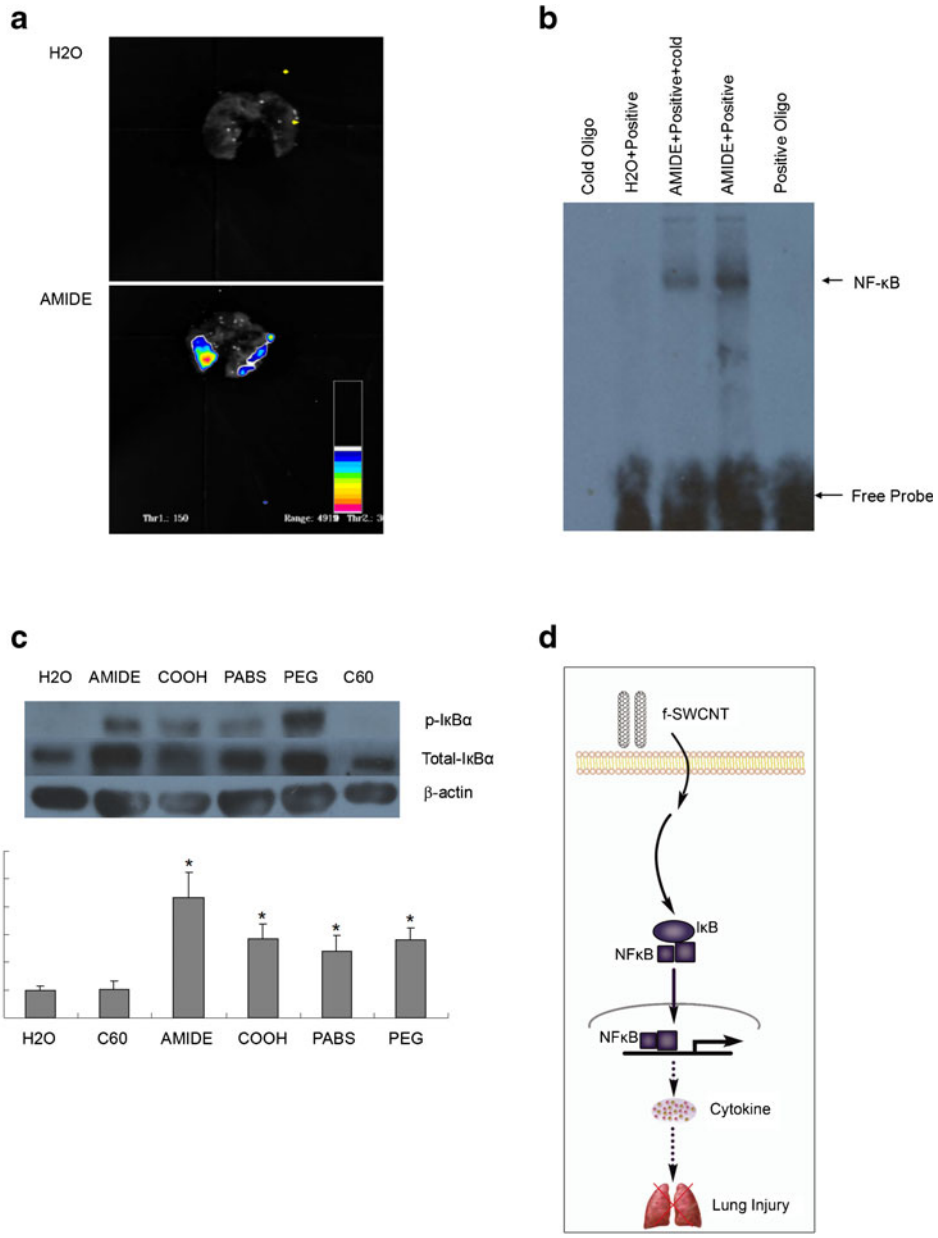

Fig. 2 The f-SWCNTs induce ALI through the NF-κB-cytokine signaling pathway. The mice were examined using the following analyses 18 h after the instillation of 10 mg/kg f-SWCNTs. **a** Bioluminescence imaging of luciferase activity in the transgenic mouse lungs. **b** EMSA results using NF-κB consensus oligonucleotides as the binding probes. **c** Representative western blotting of phosphorylated IκB levels in the BALF macrophages (*upper panel*). Total IκB was used as an internal control. The p-IκBα/total IκBα ratios were quantified by the band density scanning of the western blot images (*lower panel*), $n=4$ per group. *$P<0.05$ versus water control. **d** Schematic diagram of the NF-κB-cytokine pathway in the f-SWCNT-induced ALI

after 14 days. The total cell count, PMN cell numbers, and inflammatory cytokines in the BALF (Fig. 4a, b, e, f, and g) were all significantly decreased. The interstitial edema (Fig. 4h) detected 18 h after the instillation of 2 and 10 mg/kg AMIDE-SWCNT by the wet/dry weight ratios disappeared by day 14, as well as the changes in vascular permeability (Fig. 4i) and PaO_2 levels (Fig. 4j). These results reflected a general recovery from the ALI induced by the f-SWCNTs.

In addition to ALI, chronic inflammatory changes, lung fibrosis, and DNA damage were examined to determine the long-term toxicity of a high concentration of f-SWCNTs in mice after 2 weeks. Pathological analysis of the lung showed significantly decreased inflammatory reactions and alleviated lung lesions on day 14 (Fig. 5a, b). Representative fields in the lung histology revealed traces of macrophages that phagocytosed a large quantity of the f-SWCNTs and took on a dark brown look in the alveolar space, which was reflected in the BALF macrophage numbers peaking at day 14 in the 10 mg/kg group [Fig. 4d and 5a (lane d)]. Many of the macrophages loaded with f-SWCNTs in the day 14 cytospin preparations looked like unevenly large, round, dark brown balls, while others were much smaller and presented a blue-gray cytoplasm, suggesting that they may had just infiltrated the alveolar space. This observation shows that a considerable amount of the f-SWCNTs persists in the lung for some time and could lead to further cytotoxic effects. Multinucleated macrophages have not been found in the BALF, with the exception of a small number of double-nucleated macrophages. The lymphocyte number remained

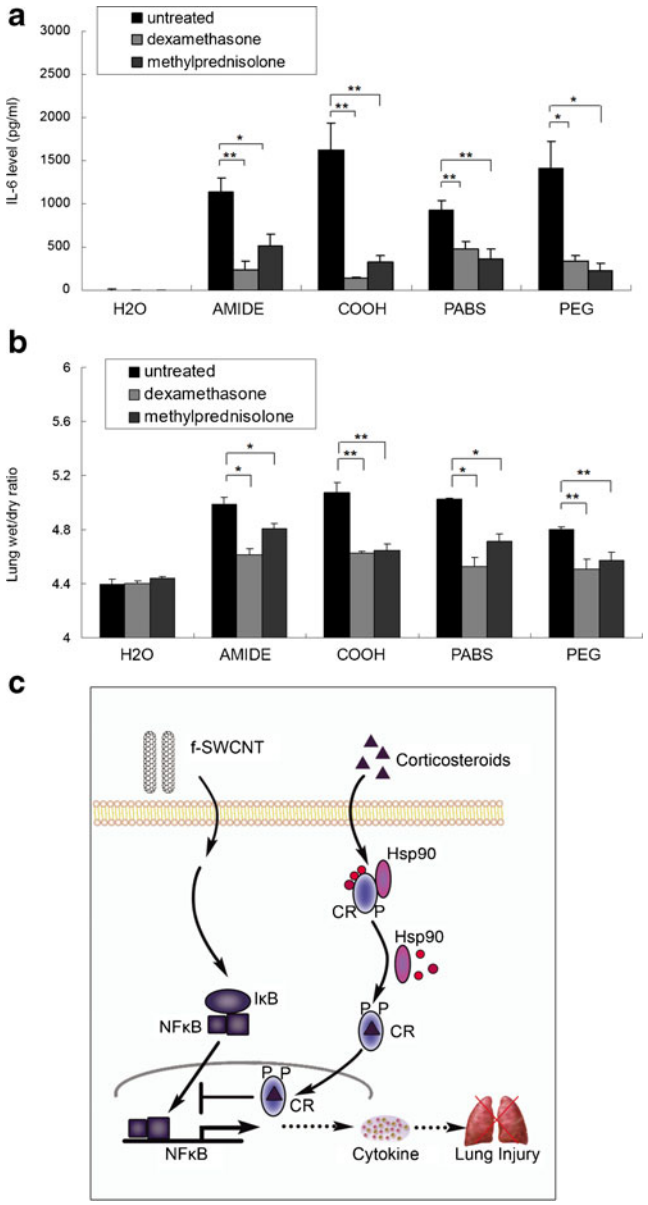

Fig. 3 Inflammation plays an important role in the f-SWCNT-induced ALI in mice. **a** BALF IL-6 concentrations. **b** Lung wet/dry ratios. Dexamethasone (10 mg/kg), methylprednisolone (50 mg/kg), or PBS was i.p. injected 1 h before mice were challenged with 10 mg/kg f-SWCNTs. *$P<0.05$, **$P<0.01$. **c** Schematic diagram of the proposed corticosteroid actions in the f-SWCNT-induced ALI

elevated in the BALF (Fig. 4c). Lungs exposed to 10 mg/kg f-SWCNTs also displayed granulomatous lesions. The COOH-SWCNT group showed the maximum value of granuloma area and number among the f-SWCNTs groups, perhaps due to the different functionalization groups in the SWCNTs [Fig. 5a (lane e), c, and d].

Lung tissue sections on day 14 after instillation were stained by Masson's trichrome, which revealed increased collagen deposition, indicated by the blue color, in the f-SWCNT groups (Fig. 5e, f). Immunohistochemistry using an anti-α-smooth muscle actin antibody was performed to identify interstitial fibroblasts or myofibroblasts, the primary effector cells that generate the extracellular matrix and offer the contractile forces during fibrogenesis. The f-SWCNT groups showed a marked increase in cells staining positive for α-SMA. Immunohistochemistry also showed excessive ECM deposition constituted by interstitial collagens, such as types I and III. The abundance ratios of collagen types I and III in the 10 mg/kg f-SWCNT-exposed lungs were higher than in the control groups (Fig. 5e, g). We also determined the extent of DNA damage using the phospho-H2A.X immunostaining assay, and the results indicated that p-H2A.X reactivity increased significantly in both the 2 and 10 mg/kg f-SWCNT-administered mice 18 h after instillation and persisted at the later time-point (Fig. 5h, i).

Discussion

Nanotechnology is developing rapidly, and awareness is growing about the potential environmental and health concerns of nanomaterials. Efforts have been made to assess the safety of these nanomaterials [1, 27]. Cases reported by Song et al. [2] arouse concern that long-term exposure to nanoparticles may be related to severe injury to human lungs. Further investigation into safety issues is urgently required.

Our present study discovered that some f-SWCNTs could induce lung toxicity in mice at an occupational exposure dose. We found that f-SWCNTs at a concentration above 0.6 mg/kg could cause signs of lung toxicity in mice. A lung burden similar to 0.6 mg/kg f-SWCNTs in mice would be achieved by human workers exposed for approximately 2 years to the peak airborne concentrations (53 $\mu g/m^3$) of f-SWCNTs in an occupational setting according to the studies of Maynard et al. [14, 22]. Mice exposed to high-dose AMIDE-SWCNT developed ALI, with symptoms of severe lung edema, enhanced pulmonary vascular permeability, and decreased PaO_2, which were mostly recovered after 14 days. The lung is apparently able to cope with a single exposure of f-SWCNTs, but we must notice that it faces a completely different challenge in terms of particle burden and stress levels in case of long term exposure. Nevertheless, our results provide an important reference for future nanomedical use and long-term occupational exposure.

The instilled f-SWCNTs were engulfed by phagocytes or taken up by other kinds of cells, and some phagocytosed f-SWCNTs might be cleared and eliminated through mucociliary clearance or other mechanisms during the post-exposure days [28]. However, the residual f-SWCNTs could persist in the lung after 14 days and might lead to adverse health effects. In certain fields with large amounts of deposited f-SWCNTs, the macrophages with phagocytosed f-SWCNTs aggregated significantly, forming granuloma-like structures

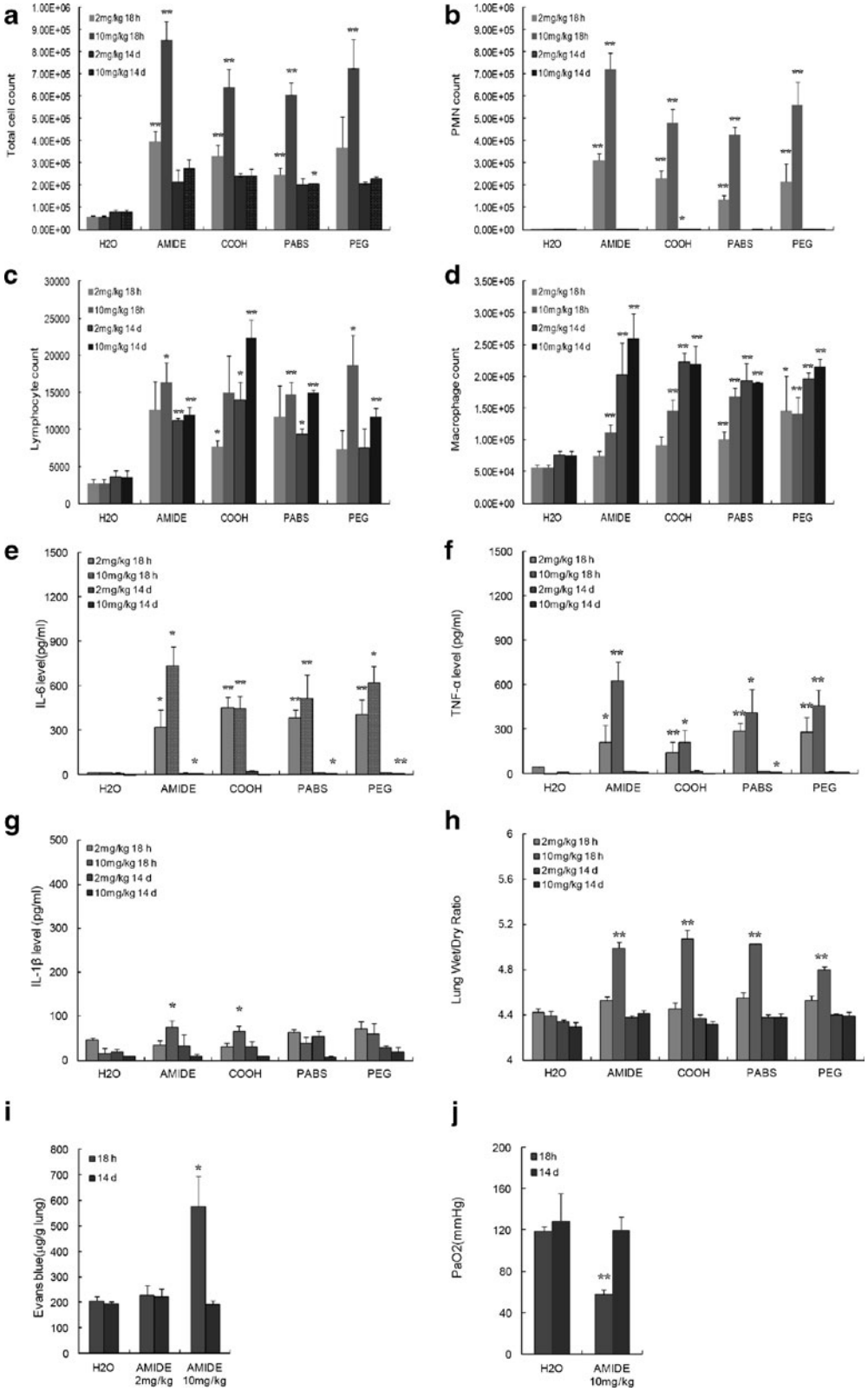

Fig. 4 BALF and functional analyses of mice 14 days after the instillation of f-SWCNTs. The mice were intratracheally given water or f-SWCNTs at 0, 2, and 10 mg/kg. **a–d** Total cell count (**a**), PMN count (**b**), lymphocyte count (**c**), and macrophage count (**d**) in the BALF using Wright–Giemsa staining under light microscopy. **e–g** ELISA analysis of the BALF: IL-6 (**e**), TNF-α (**f**), and IL-1β (**g**). **h** Lung wet/dry ratios. **i** Evans blue staining. **j** PaO_2 evaluation. The above results showed a general recovery from the ALI induced by the f-SWCNTs. n=4–6 per group. *P <0.05, **P<0.01 versus control

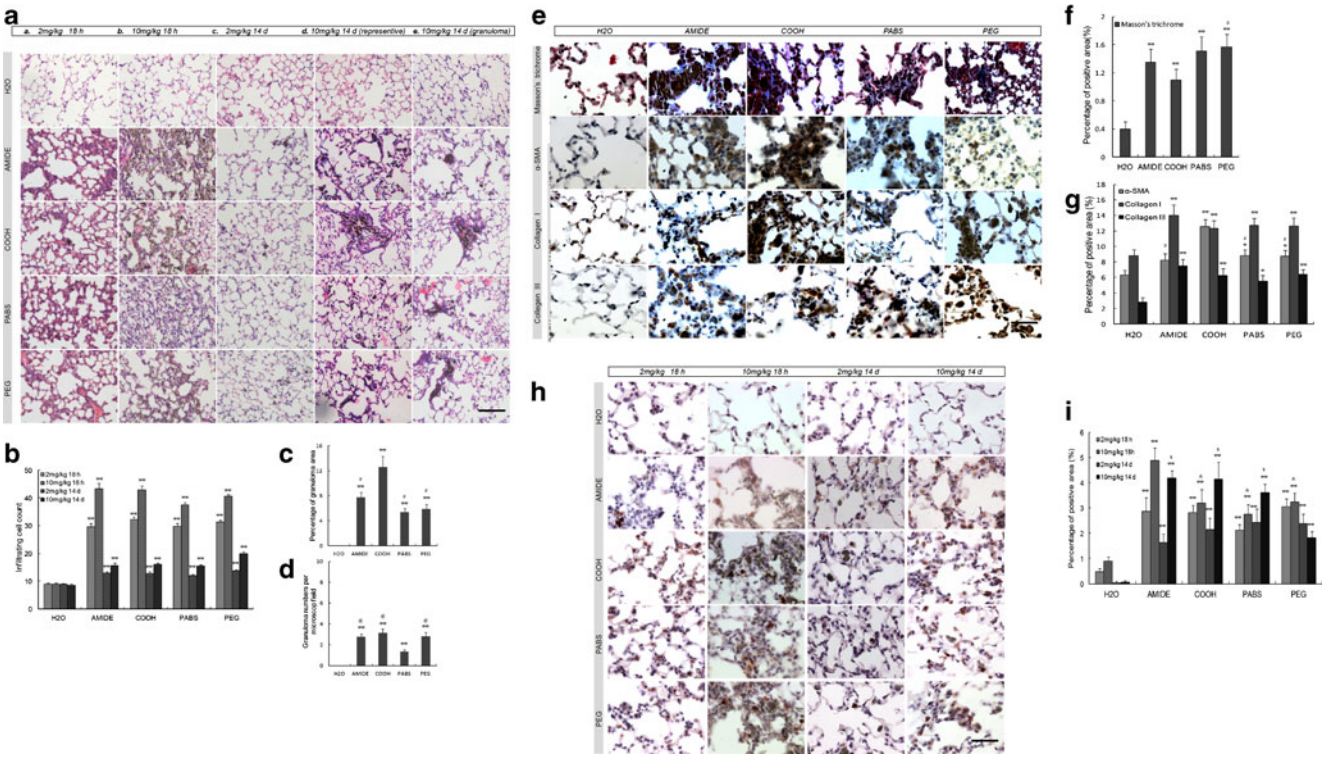

Fig. 5 Pulmonary pathologic analysis of the mice 14 days after the instillation of the f-SWCNTs. The mice were intratracheally given water or f-SWCNTs at 0, 2, and 10 mg/kg (**a**, **b**, **h**, **i**), or 0, and 10 mg/kg f-SWCNTs (**c**–**g**). **a** Representative H&E-stained lung sections from the mice. Scale bar, 100 μm. **b** Statistical analysis of the infiltrating cell numbers. **c** The percentage of granuloma area. **d** The granuloma numbers in each microscope field. **e** Mouse lung sections stained with Masson's trichrome and the fibrosis markers α-SMA, collagen I, and collagen III. Scale bar, 20 μm. **h** p-H2A.X-immunostaining of the lung sections from mice. Scale bar, 20 μm. **f**, **g**, **i** Statistical analyses of the above staining. $^{\#}P<0.05$, $^{@}P<0.05$ versus COOH-SWCNT and PABS-SWCNT, respectively. I. $^{\&}P<0.05$, $^{\$}P<0.05$ versus AMIDE-SWCNT 10 mg/kg 18 h, and PEG-SWCNT 10 mg/kg 14 days, respectively. The above results showed increased collagen staining and increased α-SMA, collagen I, collagen III, and H2A.X immunostaining in the f-SWCNT-instilled mice. $^{*}P<0.05$, $^{**}P<0.01$ versus control

that were indicative of chronic inflammation, as previously reported in aggregated pristine SWCNT-induced lung injury from 7 days postexposure [14, 15]. In such fields, we also found moderate fibrosis as demonstrated by the elevated collagen staining by Masson's trichrome and the increased immunostaining specific for α-SMA and collagens I and III. In contrast, most of the other fields showed scattered macrophages with phagocytosed f-SWCNTs and presented relatively mild lung fibrosis. Although the pathogenesis of tumor are not observed in histology, DNA damage represented by the phosphorylation of histone H2A.X at serine 139, which occurs at sites flanking DNA double strand breaks, is stained positive.

The different SWCNT modifications might play important roles in the interaction with cells and influence the toxic potential. The four differently functionalized SWCNTs generated different effects on the lung toxicity in our study. The infiltrated PMN cell counts in the BALF of the AMIDE-SWCNT dose groups higher than 0.6 mg/kg (Fig. 1d) and the H2A.X immunostaining of the 10 mg/kg AMIDE-SWCNT group (Fig. 5h, i) increased significantly at 18 h after instillation compared with the other three f-SWCNTs, which is in accordance with literatures showing that NH_{2-} modifications of NPs increase their toxicity [29, 30].This phenomenon might be correlated with the physiochemical properties of amide groups resulting in increased uptake [29–31] and dammage. Each amide function group contains one oxygen atom and one nitrogen atom, which can form plenty of hydrogen bonds with biomolecules. It is also speculated that the NH_{2-} in the amide function group, once acquiring a H^{+} to form NH_3^{+}, can damage the plasma membrane, endomembrane and DNA through direct ionic interactions with the negatively charged phospholipid, proteins, and DNA. On the other hand, COOH-SWCNT maybe the most toxic in terms of persistent lung toxicity, inducing the strongest granuloma formation according to our data (Fig. 5a, c). Although the collagen (immuno-) staining by Masson's trichrome and collagens I/III antibodies did not increase in the COOH-SWCNT group compared with the other three f-SWCNTs groups, the expression of α-SMA did increase significantly (Fig. 5e–g). α-SMA is the hallmark of myofibroblasts, which are generally considered to be

important early effector cells in the development of fibrosis; therefore, the COOH-SWCNT group might possess the strongest potential of fibrosis formation. We used dynamic light scattering (DLS) techniques to determine the f-SWCNTs' aggregate state in water and the DLS results indicated that COOH-SWCNT possessed the largest aggregate size reflected by zeta-average sizes (Table S1). COOH-SWCNT might present stronger tendency to aggregate and precipitate in vivo than the other three f-SWCNTs. The precipitated COOH-SWCNT could not be easily phagocytosed and discharged from alveolus, thus inducing the most severe granuloma formation. To summarize, we would rank the lung toxicity of the f-SWCNTs regarding acute inflammation as AMIDE-SWCNT>COOH-SWCNT>PEG-SWCNT>PABS-SWCNT, while rank that regarding sustained fibrosis as COOH-SWCNT>AMIDE-SWCNT>PEG-SWCNT>PABS-SWCNT. Our results support the notion that there are different biological effects correlating with different functionalizations and that the type of functional groups should be considered when choosing functionalized SWCNTs for nanomedicine application.

There have been numerous studies demonstrating that particle surface area is a very critical issue for particle toxicology [32, 33]. Our results suggested that f-SWCNT doses of or higher than 0.6 mg/kg (equal to 2.4 cm^2/g) induced the production of pro-inflammatory cytokines, which conformed well to the inflammation onset threshold of 20 cm^2 per mouse, demonstrated by Stoeger et al. [32], for the instilled particle surface area. The mesoporous carbon black (MCB) used in our study as reference for spherical carbon particles presented similar surface area with the ultrafine carbon black (UCB) reported [32–34]. Interestingly, MCB was much less inflammogenic than UCB [32–34]. One reason for this discrepancy might be that MCB is a mesoporous material with a mean particle size of 5 μm, while UCB is nonmesoporous nanoparticle and the particle sizes are around 14 nm. MCB contains large quantities of mesopores with diameters between 2 and 50 nm inside the particles, and the mesopore surface area occupies most of the MCB surface area. It is likely that the mesopore surface can neither directly contact nor efficiently affect the pulmonary epithelial cells and macrophages, resulting in sharply reduced particle toxicity of MCB. Therefore, we come to the proposition that particle shape feature, in addition to particle surface area, is also a very critical issue for particle toxicology.

The underlying mechanism by which the f-SWCNTs induced the proinflammatory cytokine storm was further explored. The inflammation is initiated through the activation of proinflammatory signaling cascades, with the NF-κB cascade being the most important. Although pristine SWCNTs have been reported to stimulate NF-κB activation in human keratinocytes [12] and THP-1 cells [13], along with these findings, new problems have nevertheless been brought to our attention. First, the experiments were performed in vitro, not in vivo. Second, insoluble pristine SWCNTs were used instead of functionalized ones. In our in vivo study using functionalized SWCNTs, we found activation of the NF-κB pathway at 18 h after instillation (Fig. 2). Given that we observed a continuous activation of NF-κB at 2, 4, 6, and 12 h after exposure in the EMSA experiments (Fig. S2), this activation might have started during the very early hours and launched the kinetics of inflammation while remaining upregulated until 18 h and longer. In short, our study indicated that the f-SWCNTs induced ALI in mice through the activation of the NF-κB-cytokine pathway.

Corticosteroids are clinically effective in the treatment of ALI or ARDS by decreasing inflammation and inhibiting the activity of the immune system [25]. Many anti-inflammatory actions of corticosteroids are attributed to the disruption of NF-κB function, which is also confirmed in our EMSA result of corticosteroid treatment (Fig. S3). The corticosteroid receptor represses the transcriptional activity of NF-κB by physically interacting with p65 in addition to other mechanisms (Fig. 3c, right pathway) [35]. Our data showed not only that doses of f-SWCNTs higher than 0.6 mg/kg induced ALI by causing excessive systemic inflammation, leading to the ALI in the mice, but also that corticosteroids could inhibit the f-SWCNT-induced ALI in vivo through suppression of the proinflammatory cytokine production induced by NF-κB activation (Fig. 3c).

In this report, we show that instillation of f-SWCNTs in mice could induce ALI with inflammatory reactions. We elucidate that signaling through the NF-κB-cytokine pathway is responsible for the ALI caused by pulmonary exposure to f-SWCNTs in vivo. Moreover, we discovered that corticosteroids could be used to treat excessive inflammation in the lung in case of an unintentional exposure to f-SWCNTs, suggesting a potential clinically available remedy for nanoparticle-induced lung injury. Finally, we evaluated the self-repair ability and chronic inflammation of the mouse lung on day 14. The ALI was almost completely reversed within 14 days, but mild to moderate fibrosis, granuloma, and DNA damage remained in the mice at day 14. Most important of all, we found that the four differently functionalized SWCNTs generated different effects on the lung toxicity, and ranked AMIDE-SWCNT and COOH-SWCNT the first, respectively, for acute and chronic lung toxicity.

Acknowledgments The authors thank Xiangwu Ju for help with the illustrations and gratefully acknowledge Prof. Haiyan Xu, Dr. Jie Meng, Dr. Jian Liu, Weiqi Zhang, and Peng Zhang for their helpful suggestions and kind assistance. This work was supported by the National Natural Science Foundation of China (30625013 and

30721063) and the Ministry of Science and Technology of China (2009ZX10004-308, 2009CB522105, and 2011CB933504).

Disclosure The authors declare no conflict of interest related to this study.

References

1. Xia T, Li N, Nel AE (2009) Potential health impact of nanoparticles. Annu Rev Public Health 30:137–150
2. Song Y, Li X, Du X (2009) Exposure to nanoparticles is related to pleural effusion, pulmonary fibrosis and granuloma. Eur Respir J 34:559–567
3. Pope CA 3rd, Ezzati M, Dockery DW (2009) Fine-particulate air pollution and life expectancy in the United States. N Engl J Med 360:376–386
4. Kostarelos K, Bianco A, Prato M (2009) Promises, facts and challenges for carbon nanotubes in imaging and therapeutics. Nat Nanotechnol 4:627–633
5. Bianco A, Kostarelos K, Prato M (2005) Applications of carbon nanotubes in drug delivery. Curr Opin Chem Biol 9:674–679
6. Chen J, Chen S, Zhao X, Kuznetsova LV, Wong SS, Ojima I (2008) Functionalized single-walled carbon nanotubes as rationally designed vehicles for tumor-targeted drug delivery. J Am Chem Soc 130:16778–16785
7. Witzmann FA, Monteiro-Riviere NA (2006) Multi-walled carbon nanotube exposure alters protein expression in human keratinocytes. Nanomedicine 2:158–168
8. Ryman-Rasmussen JP, Cesta MF, Brody AR, Shipley-Phillips JK, Everitt JI, Tewksbury EW, Moss OR, Wong BA, Dodd DE, Andersen ME et al (2009) Inhaled carbon nanotubes reach the subpleural tissue in mice. Nat Nanotechnol 4:747–751
9. Bai Y, Zhang Y, Zhang J, Mu Q, Zhang W, Butch ER, Snyder SE, Yan B (2010) Repeated administrations of carbon nanotubes in male mice cause reversible testis damage without affecting fertility. Nat Nanotechnol 5:683–689
10. Liu Z, Chen K, Davis C, Sherlock S, Cao Q, Chen X, Dai H (2008) Drug delivery with carbon nanotubes for in vivo cancer treatment. Cancer Res 68:6652–6660
11. Ruggiero A, Villa CH, Bander E, Rey DA, Bergkvist M, Batt CA, Manova-Todorova K, Deen WM, Scheinberg DA, McDevitt MR (2010) Paradoxical glomerular filtration of carbon nanotubes. Proc Natl Acad Sci USA 107:12369–12374
12. Manna SK, Sarkar S, Barr J, Wise K, Barrera EV, Jejelowo O, Rice-Ficht AC, Ramesh GT (2005) Single-walled carbon nanotube induces oxidative stress and activates nuclear transcription factor-kappaB in human keratinocytes. Nano Lett 5:1676–1684
13. Chou CC, Hsiao HY, Hong QS, Chen CH, Peng YW, Chen HW, Yang PC (2008) Single-walled carbon nanotubes can induce pulmonary injury in mouse model. Nano Lett 8:437–445
14. Shvedova AA, Fabisiak JP, Kisin ER, Murray AR, Roberts JR, Tyurina YY, Antonini JM, Feng WH, Kommineni C, Reynolds J et al (2008) Sequential exposure to carbon nanotubes and bacteria enhances pulmonary inflammation and infectivity. Am J Respir Cell Mol Biol 38:579–590
15. Lam CW, James JT, McCluskey R, Hunter RL (2004) Pulmonary toxicity of single-wall carbon nanotubes in mice 7 and 90 days after intratracheal instillation. Toxicol Sci 77:126–134
16. Delogu LG, Venturelli E, Manetti R, Pinna GA, Carru C, Madeddu R, Murgia L, Sgarrella F, Dumortier H, Bianco A (2012) Ex vivo impact of functionalized carbon nanotubes on human immune cells. Nanomedicine (Lond) 7:231–243
17. Zhang Y, Xu Y, Li Z, Chen T, Lantz SM, Howard PC, Paule MG, Slikker W Jr, Watanabe F, Mustafa T et al (2011) Mechanistic toxicity evaluation of uncoated and PEGylated single-walled carbon nanotubes in neuronal PC12 cells. ACS Nano 5:7020–7033
18. Patlolla A, McGinnis B, Tchounwou P (2011) Biochemical and histopathological evaluation of functionalized single-walled carbon nanotubes in Swiss–Webster mice. J Appl Toxicol 31:75–83
19. Konduru NV, Tyurina YY, Feng W, Basova LV, Belikova NA, Bayir H, Clark K, Rubin M, Stolz D, Vallhov H et al (2009) Phosphatidylserine targets single-walled carbon nanotubes to professional phagocytes in vitro and in vivo. PLoS One 4: e4398
20. Tong H, McGee JK, Saxena RK, Kodavanti UP, Devlin RB, Gilmour MI (2009) Influence of acid functionalization on the cardiopulmonary toxicity of carbon nanotubes and carbon black particles in mice. Toxicol Appl Pharmacol 239:224–232
21. Liu HL, Zhang YL, Yang N, Zhang YX, Liu XQ, Li CG, Zhao Y, Wang YG, Zhang GG, Yang P et al (2011) A functionalized single-walled carbon nanotube-induced autophagic cell death in human lung cells through Akt-TSC2-mTOR signaling. Cell Death Dis 2: e159
22. Maynard AD, Baron PA, Foley M, Shvedova AA, Kisin ER, Castranova V (2004) Exposure to carbon nanotube material: aerosol release during the handling of unrefined single-walled carbon nanotube material. J Toxicol Environ Health A 67:87–107
23. Schanen BC, Karakoti AS, Seal S, Drake DR 3rd, Warren WL, Self WT (2009) Exposure to titanium dioxide nanomaterials provokes inflammation of an in vitro human immune construct. ACS Nano 3:2523–2532
24. Adcock IM, Caramori G, Ito K (2006) New insights into the molecular mechanisms of corticosteroids actions. Curr Drug Targets 7:649–660
25. Tang BM, Craig JC, Eslick GD, Seppelt I, McLean AS (2009) Use of corticosteroids in acute lung injury and acute respiratory distress syndrome: a systematic review and meta-analysis. Crit Care Med 37:1594–1603
26. Tyburski JG, Dente C, Wilson RF, Steffes C, Devlin J, Carlin AM, Flynn LM, Shanti C (2001) Differences in arterial and mixed venous IL-6 levels: the lungs as a source of cytokine storm in sepsis. Surgery 130:748–751, discussion 751-742
27. Nel A, Xia T, Madler L, Li N (2006) Toxic potential of materials at the nanolevel. Science 311:622–627
28. Mutlu GM, Budinger GR, Green AA, Urich D, Soberanes S, Chiarella SE, Alheid GF, McCrimmon DR, Szleifer I, Hersam MC (2010) Biocompatible nanoscale dispersion of single-walled carbon nanotubes minimizes in vivo pulmonary toxicity. Nano Lett 10:1664–1670
29. Bhattacharjee S, de Haan LH, Evers NM, Jiang X, Marcelis AT, Zuilhof H, Rietjens IM, Alink GM (2010) Role of surface charge and oxidative stress in cytotoxicity of organic monolayer-coated silicon nanoparticles towards macrophage NR8383 cells. Part Fibre Toxicol 7:25
30. Xia T, Kovochich M, Brant J, Hotze M, Sempf J, Oberley T, Sioutas C, Yeh JI, Wiesner MR, Nel AE (2006) Comparison of the abilities of ambient and manufactured nanoparticles to induce cellular toxicity according to an oxidative stress paradigm. Nano Lett 6:1794–1807
31. Kim BY, Jiang W, Oreopoulos J, Yip CM, Rutka JT, Chan WC (2008) Biodegradable quantum dot nanocomposites enable live

cell labeling and imaging of cytoplasmic targets. Nano Lett 8:3887–3892
32. Stoeger T, Reinhard C, Takenaka S, Schroeppel A, Karg E, Ritter B, Heyder J, Schulz H (2006) Instillation of six different ultrafine carbon particles indicates a surface area threshold dose for acute lung inflammation in mice. Environ Health Perspect 114:328–333
33. Sager TM, Castranova V (2009) Surface area of particle administered versus mass in determining the pulmonary toxicity of ultrafine and fine carbon black: comparison to ultrafine titanium dioxide. Part Fibre Toxicol 6:15
34. Dick CA, Brown DM, Donaldson K, Stone V (2003) The role of free radicals in the toxic and inflammatory effects of four different ultrafine particle types. Inhal Toxicol 15:39–52
35. Necela BM, Cidlowski JA (2004) Mechanisms of glucocorticoid receptor action in noninflammatory and inflammatory cells. Proc Am Thorac Soc 1:239–246